ISSN 8755-6839

SCIENCE OF TSUNAMI HAZARDS

Journal of Tsunami Society International

Volume 35 Number 3 2016

ENHANCED VERTICAL EVACUATION APPLICATION WITH GEOMATIC TOOLS FOR TSUNAMIS IN SALINAS, ECUADOR

Andres Sebastian Matheus Medina, Mario Cruz D´Howitt, Oswaldo Padilla Almeida, Theofilos Toulkeridis* and Ana Gabriela Haro

Universidad de las Fuerzas Armadas ESPE, Sangolquí, Ecuador

*** Corresponding author:** ttoulkeridis@espe.edu.ec **or** theousfq@yahoo.com

ABSTRACT

Tsunami hazards are more than evident in the Pacific coast of Ecuador, but especially on its westernmost Peninsula called Salinas. As the potential impact time is relatively short for the public to reach natural high ground or at least leave the tsunami inundation area, a different approach to rescue lives has been applied with geomatic tools. The buildings inside the tsunami hazard zone have been first evaluated for their seismic resistance. Those buildings, which have been proven to withstand a seismic event, have been chosen to serve as elevated safe zones for a subsequent vertical tsunami evacuation. The used geographic tools allowed reducing time spans between initial evacuation points towards safe zones inside the tsunami inundation areas. The results of this study demonstrate the efficiency of vertical tsunami evacuation in a highly populated and visited touristic area in coastal Ecuador, as in Salinas appears a relatively high percentage of the population to far from shelters or elevated safe zones during a short-time impact of a tsunami.

Key words: *Tsunami, Seismic resistant buildings, Numerical modeling, Vertical Evacuation, Ecuador*

1. INTRODUCTION

Among earthquakes and floods, tsunamis are one of the most destructive and deadliest natural hazards (Raschky, 2008; Daniell et al., 2010). In recent years many studies have been performed to demonstrate and evaluate the vulnerability of coastal cities of short-warning impacts of potentially devastating tsunamis (Walters, and Goff, 2003; Dominey-Howes, and Papathoma, 2007; Taubenböck et al., 2009; Steinmetz et al., 2010). Therefore, the implementation of evacuation signs and routes for the survival of coastal areas vulnerable of the probable impact of tsunamis is a fundamental aspect of risk assessment (Johnston et al., 2005; Yeh et al., 2005; Jonientz-Trisler et al., 2005; Dengler, 2005). However, even when evacuation routes are assigned, still people who try to escape towards higher ground or outside the flooding zones, may do not reach such safe areas prior the impact of a tsunami or due to short warning times (Xie et al., 2012; Park et al., 2012). For such circumstances, it is recommended to apply vertical evacuation of in-situ-shelters, which themselves are resistant to the seismic event and the incoming tsunami (Reese et al., 2007; FEMA, 2008; Fraser et al., 2012; Muhari et al., 2012; Mas et al., 2013; Velotti et al., 2013; Wood et al., 2014).

The main aim of this research has been to demonstrate the efficiency of vertical tsunami evacuation in a highly populated and visited touristic area in coastal Ecuador, as in Salinas appears a relatively high percentage of the population to far from shelters or elevated safe zones during a short-time impact of a tsunami. The geographic tools used shall allow to reduce time spans between evacuation points towards safe zones outside the tsunami inundation areas and where applicable towards higher seismic resistant elevations within the hazard zones.

2. GEODYNAMIC SETTING

The Ecuadorian active continental platform is a frequent target of tsunamis due to the subduction of the oceanic Nazca Plate with the continental South American and Caribbean Plates, both separated by the Guayaquil-Caracas Mega Shear (Kellogg and Vega, 1995; Gutscher et al., 1999; Gusiakov, 2005; Egbue and Kellog, 2010; Pararas-Carayannis, 2012). Furthermore, in the same area tsunamis are generated not only from the mentioned tectonic origin but also due to enormous mass failures generating submarine landslides (Shepperd and Moberly, 1981; Pontoise and Monfret, 2004; Ratzov et al, 2007; 2010; Ioualalen et al., 2011; Pararas-Carayannis, 2012). A further origin of tsunamis has been credited to the Galápagos volcanism (Toulkeridis, 2011).

The Ecuadorian shoreline has witnessed a dozen times impacts of tsunamis (Fig. 1; 2) by mainly local origins in the last two centuries with various intensities one being of up to 8.8 Mw in 1906 (Rudolph and Szirtes, 1911; Kelleher, 1972; Beck and Ruff, 1984; Kanamori and McNally, 1982; Swenson and Beck, 1996; Pararas-Carayannis, 2012; Toulkeridis et al., 2016a; Rodriguez et al., 2016), while evidences of paleo-tsunami deposits are scarce (Chunga and Toulkeridis, 2014). Other prominent examples of tsunamis along the Ecuador–Colombia subduction zone include tsunamis in 1942 (Mw=7.8), 1958 (Mw=7.7), 1979 (Mw=8.2) and 2016 (Mw=7.8) within the 600-km long rupture area of the great 1906 event (Collot et al., 2004; Toulkeridis et al., 2016a; b). While the 1906 event caused the death of up to 1500 persons in Ecuador and Colombia, the 1979 tsunami killed in Colombia at least 807 persons (Pararas-Carayannis, 1980). The evaluation of the last marine quakes, which generated tsunamis, suggests that the probability of a major or great earthquake in this margin region is enormous, especially as there must be substantial strain accumulation (Pararas-Carayannis, 2012).

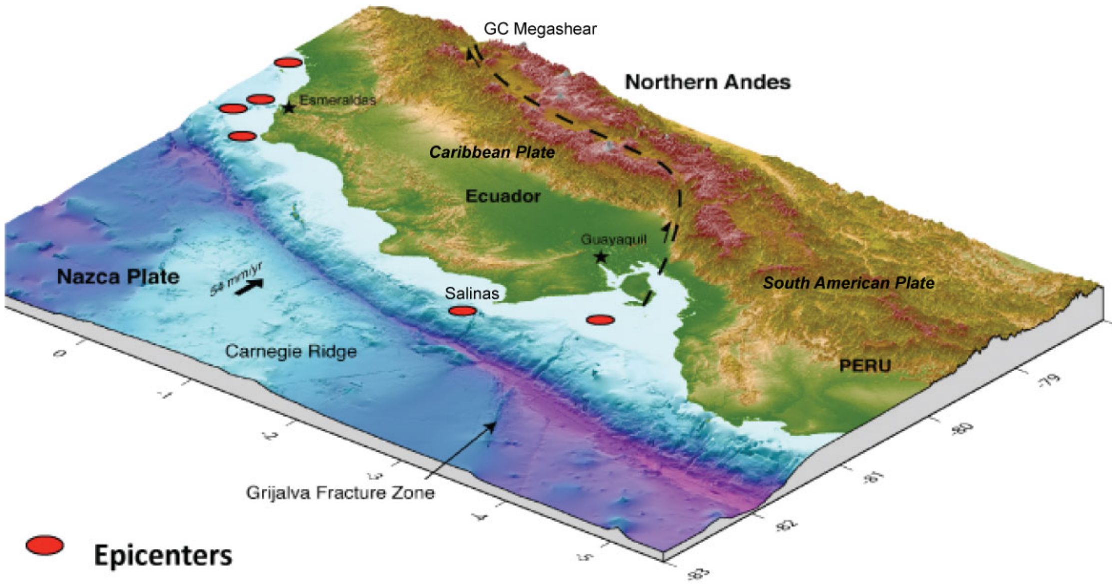

Fig. 1: Panoramic view of the morphology of western Ecuador and location of seismic epicenters, which generated tsunamis in the last 110 years. Adapted and modified from Collot et al., 2004.

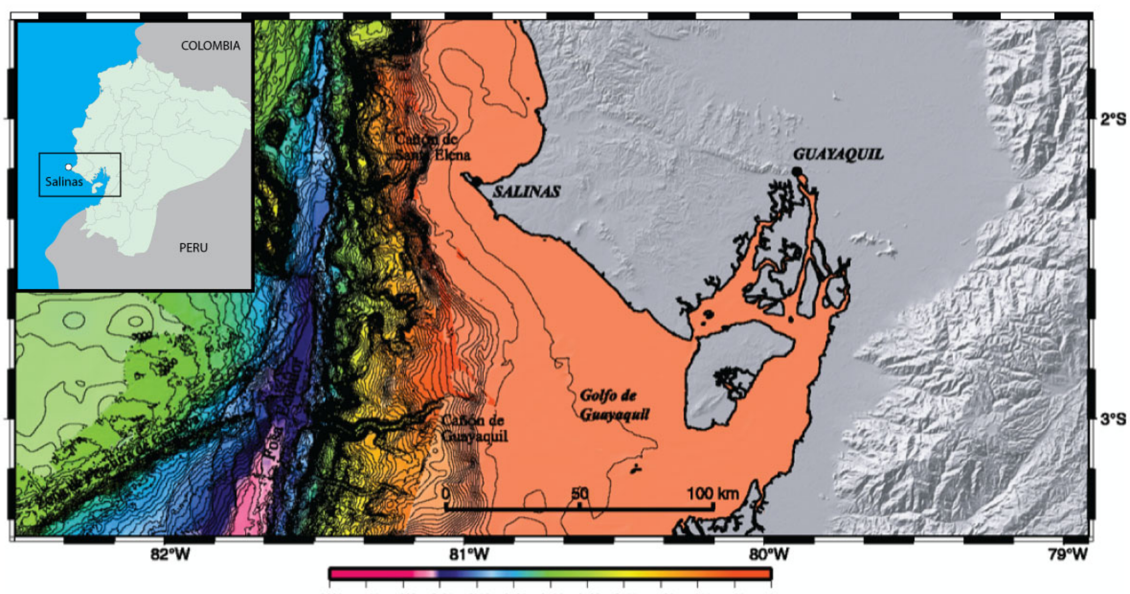

Fig. 2: Bathymetric map and location of Salinas. Adapted and modified from Collot et al., 2004.

3. TSUNAMI HAZARD IN SALINAS

The city of Salinas is part of the Santa Elena peninsular and is the most visited touristic area for its beaches and hotel infrastructure in Ecuador (Fig. 2; 3). Based on the last census of 2010, the population of the peninsula reaches some 281,467 persons and receives some 200,000 visitors at high seasons, which means that the area reaches a usual density of some 1082,22 persons per km^2 (27,07 km^2) in the urban area and up to 2,164,47 persons per km^2 at high seasons. Salinas will suffer serious damages when a tsunami will occur because the city is situated practically at sea level, except for the "Loma Lighthouse" where a military zone has been established being at some 80 m.a.s.l. The second elevated safe zone being relatively accessible for the neighborhoods around the Hotel Barceló Miramar is "Petropolis", an oil field located between Salinas and Santa Rosa. That mans, that the calculated flood area cover almost the entire city of Salinas, including the hotel and commercial infrastructure as well as great part of the military zone (Fig. 4a).

Fig. 3: Aerial view of the beach, hotel and commercial area of Salinas.

The Peninsula is exclusively composed by quaternary sediments of the so-called Tablazo formation above some minor outcrops of Cretaceous ophiolites of the Cayo Formation (Olsson, 1931; Senn, 1940) and it is situated along the Ecuador–Colombia subduction zone, at alatitude of 2.10ºS (Fig. 2, 4, 5). As the Santa Elena Peninsula is the westernmost continental spot of Ecuador, a tsunami that may be triggered in this active tectonic zone will reach Salinas in just a few minutes (Padilla et al., 2009).

therefore this sector becomes a critical and highly vulnerable area (Fig. 5 a b). Due to these circumstances, an alternative form of potential survival for the public may be the vertical evacuation in buildings, which themselves are considered seismic-resistant.

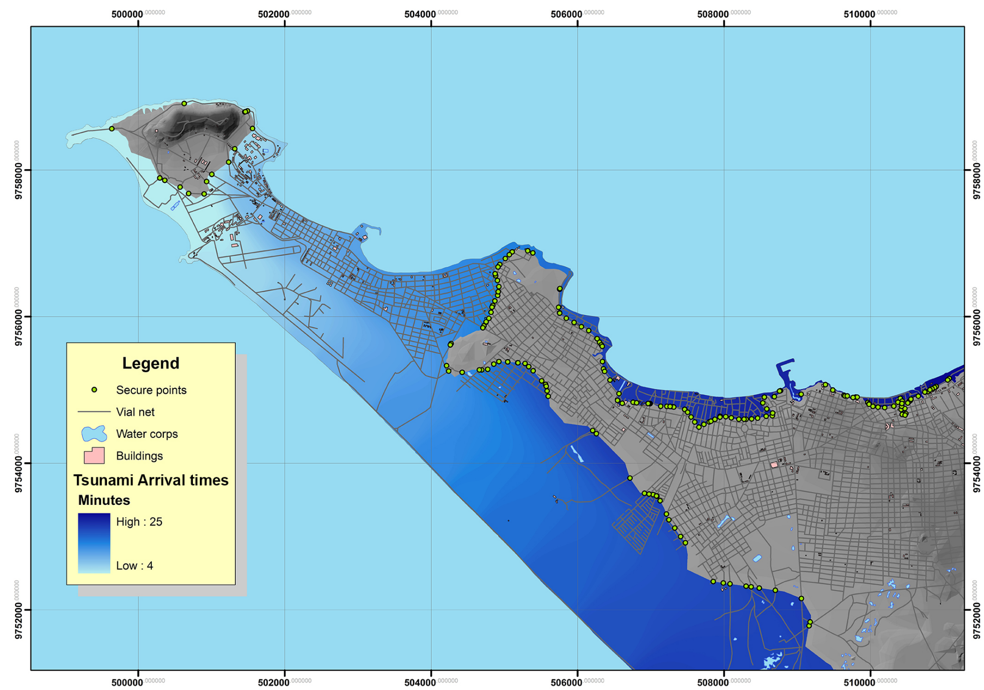

Fig. 4: Tsunami arrival times of Salinas.

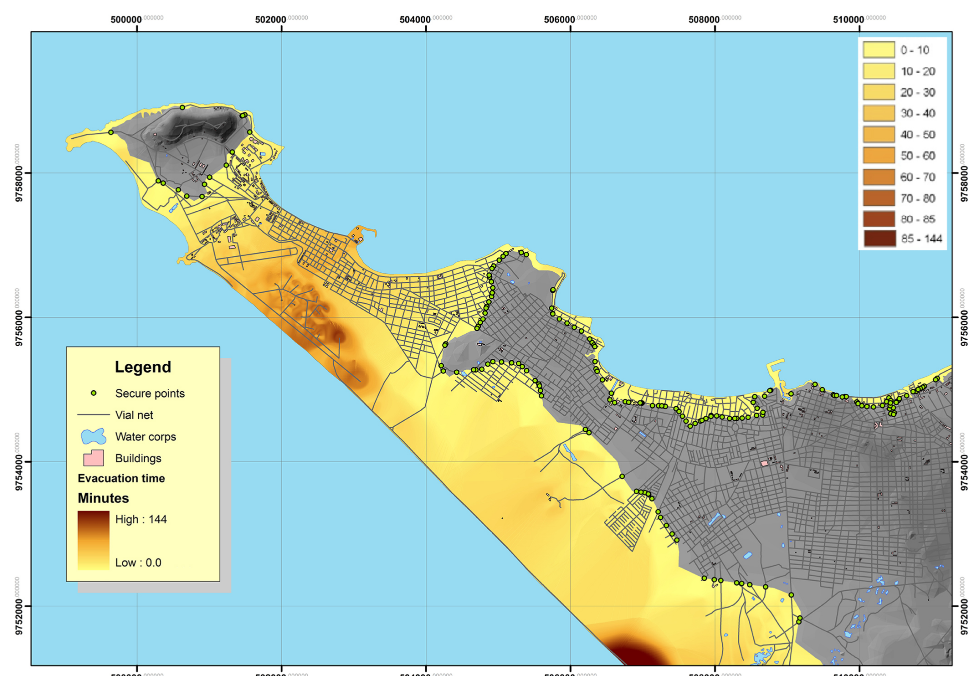

Fig. 4: Tsunami Evacuation times in Salinas.

4. METHODOLOGY

4.1 Seismic resistance

Vertical evacuation refuges from tsunamis are valuable risk-reduction facilities for highly populated regions where higher ground zones are not accessible or where arrival times of tsunami waves are short (Wood et al. 2014). A previously conducted study concluded that the first tsunami wave would strike Salinas in 8 to 12 minutes being around six meters high (Padilla et al., 2009; Matheus, 2012). Therefore, Salinas is an ideal place where vertical evacuation needs to be considered due to its location and geomorphological conditions. In this respect to withstand tsunami forces, and elevate evacuees above the maximum expected tsunami wave height (FEMA 2008), a tsunami vertical evacuation shelter is a building or earthen mound designed and constructed to withstand tsunami forces, and elevate evacuees above the maximum expected tsunami wave height (FEMA 2008).

Building a structure for a vertical evacuation shelter may cost up to 20% more than a building without tsunami preventive construction techniques. Instead, existing heavy constructions such as reinforced concrete buildings may be considered as potential tsunami shelters once detailed structural analyses are conducted to establish if the structures are capable of withstanding ground motions and forces associated with tsunamis waves (FEMA 2012). A tsunami vertical evacuation shelter must be designed to resist the generating earthquake plus eight different types of tsunami forces: (1) hydrostatic forces; (2) buoyant forces; (3) hydrodynamic forces; (4) impulsive forces; (5) debris impact forces; (6) debris damming forces; (7) uplift forces; and, (8) additional gravity loads from retained water on elevated floors (FEMA, 2008).

Regarding the structure, ductile and redundant systems that remain functional after an earthquake are required. Additionally, open systems that offer minimum resistance to water flow, and strong and deep foundations play an important role when choosing an appropriate structural configuration for a vertical evacuation facility. Reinforced concrete moment resisting frame buildings and structural wall systems with their walls parallel to the predicted wave flow accomplish these conditions. Accessibility for individuals with physical disabilities should also be considered when selecting on a vertical evacuation facility.

Our study has been conducted to identify possible vertical evacuation buildings / shelters in Salinas. The survey included a total of 61 buildings inspected. Considering most of the criteria described above and a minimum number of stories equal to five, only seven buildings in Salinas were selected as potential vertical evacuation shelters (Fig. 6). Once these buildings have been selected, a second phase of the study would consist of performing detailed structural evaluations to verify if the buildings are certainly capable of withstanding strong ground shakings according to the Ecuadorian Construction Standards NEC-15 and the described forces originated from a tsunami (NEC-15, 2015).

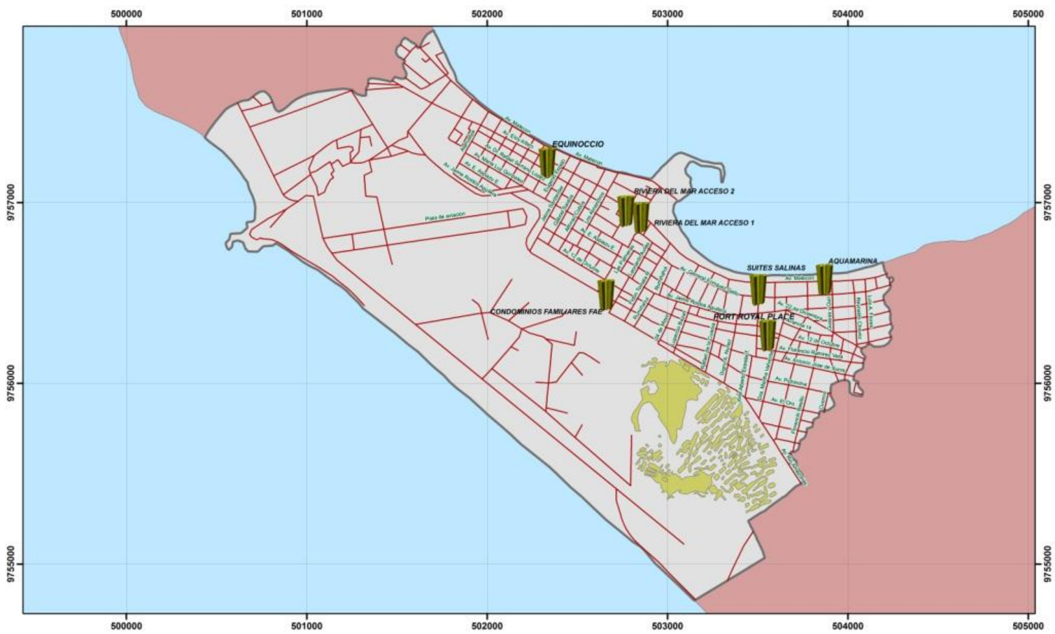

Figure 6: Potential vertical evacuation shelters on seismic resistant buildings in Salinas.

Such vertical evacuation shelters in addition to be earthquake resistant features, they have wide access, which will allow the rise of the evacuees safely and relatively quickly. The streets and avenues that can reach each security checkpoints are in good condition, are spacious and have no congestion by automotive traffic, which would provide a good value access to areas near these points.

4.2 Modelling the vertical evacuation accessibility

Based on the mentioned consideration about limited evacuation times and accesses, we have considered to evaluate and apply vertical evacuation as a plausible alternative towards the potential tsunami hazard. Once we have identified which buildings are considered to be safe, the next step has been the creation of scenarios for different evacuation times, for the subsequent determination of the coverage areas of each building. Within such we need to identify the accessibility values, times of mobilization and determine the optimal evacuation routes.

4.2a Methodology to determine evacuation scenarios

Time is always crucial when different scenarios are generated. In case of using an immediate evacuation, the time factor determines the amount of people who may be able to be saved from the tsunami hazard. In a representative building with 10 floors, we took the time a person needs to access the uppest terrace starting from the opposite sidewalk. In order to have unbiased information of such race, we have chosen four persons with different characteristics of gender, age and health status (Table 1).

Table 1: Times of ascent. Awareness is the addition of one minute to the taken time for the ascent. The 2´38´´is the average time of the first three persons

	Gender	Age	Physical condition	Time	Awareness
Person 1	Female	23 years	good	1´40´´	2´38´´
Person 2	Male	26 years	good	1´20´´	
Person 3	Male	50 years	good	1´54´´	
Person 4	Male	55 years	bad	2´40´´	3´40´´

As indicated in Table 1, the times obtained by the first three people determined a difference of about 34 seconds between them, while the fourth person obtained a very remote time related to the others. Therefore, it has been decided to average the first three times and have a second time value obtained by the fourth person of the ascent towards the security areas. These are, at least the fifth floor of the buildings that function as security points. To the obtained times we added one extra minute which would be the time range calculated for a person to react about the psychological impact caused by the earthquake and or activation of a tsunami warning (Table 1). The values obtained were subtracted from the times of the arrival of the first tsunami wave and thus the different scenarios of times in order to reach safe areas (Table 2). These and other data and parameters were used to obtain evacuation maps as illustrated methodology of in Fig. 7**.**

Table 2: Impact time and corresponding scenarios for the city of Salinas

	Arrival of tsunami (T)	Arrival in safe zone (T)	Total (T)
Scenario 1	11´	2´38´´	8´22´´
Scenario 2	11´	3´40´´	7´20´´

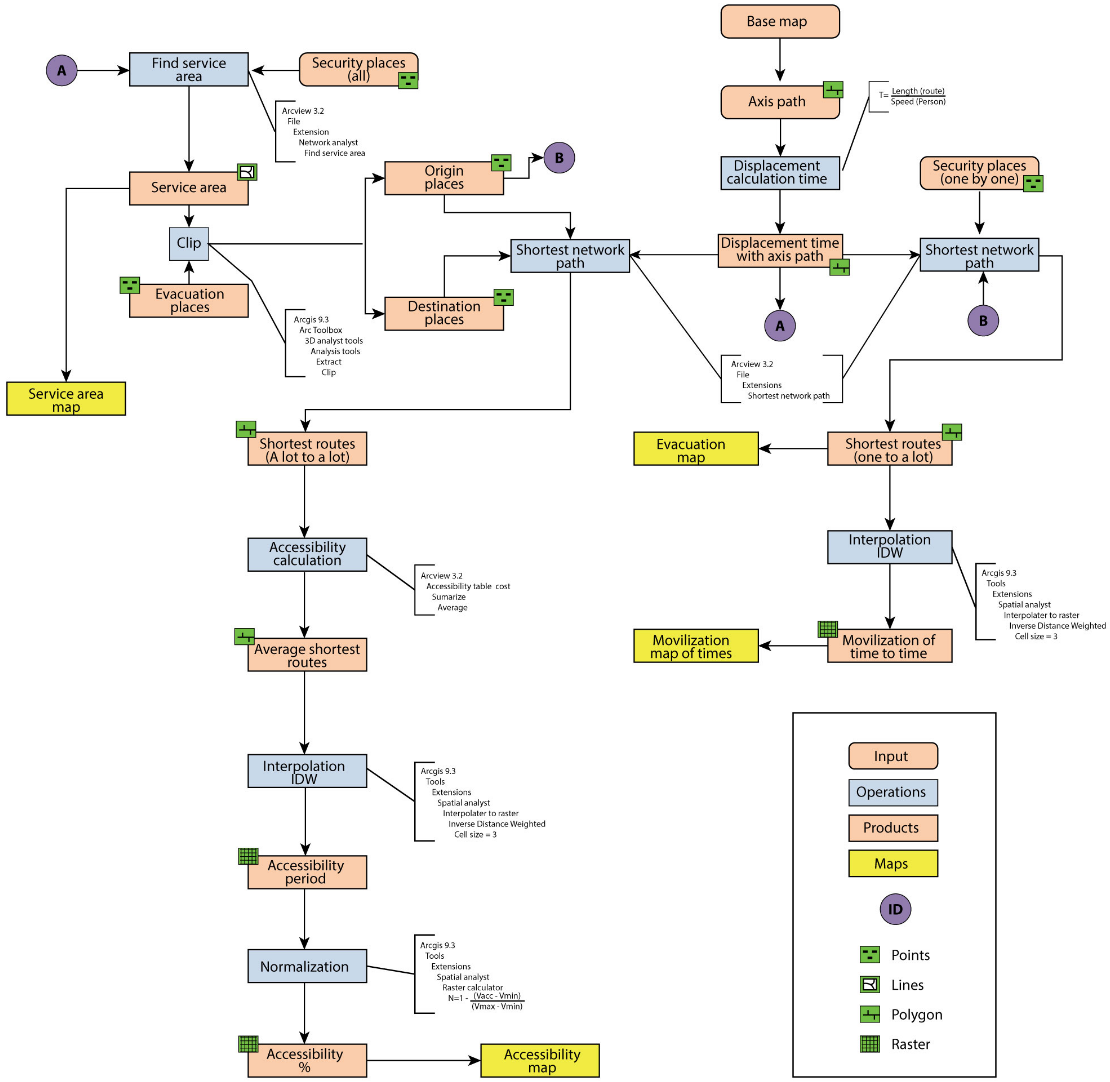

Fig. 7: Methodology to obtain maps due to a vertical evacuation model

4.2b Determination evacuation coverage areas (ECA)

In order to obtain the coverage areas of each safe area or site, the road network with a field showing all times impedance of each track segment were needed. These were elaborated with basic tools of Arcgis^{TM}, and the application Clip^{TM}. With these applications we proceeded to recalculate the mobilization times for each road segment, for which two new fields were created in the attribute table of coverage of roads, called: RECALC_MIN and speed. In the second field the velocity data were entered with the given parameter of which people move on foot in an emergency being equivalent to 150m / minute (FEMA, 2008).

The field "RECALC MIN" I was assigned for values through the Field Calculator tool, using the following formula:

Where,

Length: Distance in meters of each road segment.
Speed: Speed, expressed in meters per minute at which people move walking.
Impedance: Value of penalty that is given to each track according to obstacles or facilities being provided while using it.

With such calculation we obtained the mobilization times of the main road or path axes. For the following process we loaded the coverages of the safe areas and sites and the recently modified road network. Network analysis was performed using the tool allowing us to determine the coverage area for each evacuation safe area. While the tool has been deployed we proceeded to enter the safe area points and values of the scenarios, of which we seeked to obtain the coverage areas of each point. We further proceeded to resolve the function and coverage area for each safe area site, expressed as a polygon. With the obtained coverage polygons, we used editing tools in order to delimit the polygons avoiding any overlap of their areas to each other. The criteria we have used for the delimitation has been capacity of reception of each safe site.

4.2c Shortest ways

Only the evacuation points (input), that were situated within each coverage area using the Clip™ tool were extracted. With the layer of the evacuation points of each coverage area a new network analysis through GIS has been realized. With that we were able to determine the shortest route between two points coverages, with the time expressed in minutes being a determining factor. In order to obtain the mobilization times, we entered the coverage evacuation points and they were compared versus the safety point of each coverage area. After performing this process a new linear coverage of the most optimal routes was obtained with a corresponding table attribute.

The same procedure was performed to obtain accessibility times, with the difference that this time we entered and compared the coverage evacuation points versus the coverage destination points, which, for purposes of understanding represent the identical points. Consequently the routes coverage were obtained with their table attributes. With this linear coverage of the shortest routes, we elaborated the different evacuation route maps for each coverage area. From this point on, different procedures were determined to obtain the models of mobilization times and accessibility, pending on the methodology used.

4.2d Mobilization time model

With the tool Join™ we related the data in the table with the mobilization times with the attribute table coverage evacuation points (input) by the common field EVT_ID. By obtaining the mobilization timesheets corresponding to a coverage point, we proceeded to perform an interpolation using the

Inverse Distance Weighting method. The parameters for the tool to perform the process were entered, and the mobilization time model has been obtained.

4.2e Accessibility model

For an accessibility model, the average time of accessibility obtained before has been obtained by applying the equation:

$$Accesibility=Times\ of\ mobility\ (from\ each\ initial\ evacuation\ point\ until\ safe\ site)Number\ of\ evacuation\ point$$

The table data were related with the average times of accessibility, with the attribute table coverage evacuation points (input) by the common EVT_LABEL, while using Join™. By receiving the timesheets accessibility corresponding to a coverage point, we proceeded to perform an interpolation using the Inverse Distance Weighting method. The parameters for the tool to perform the process were entered, and the mobilization time model has been obtained.
Unlike the model of mobilization times, accessibility values were expressed as a percentage, for which we proceeded to normalize the values of coverage using the Raster Calculator tool, applying the following equation:

$$Accesibility=1-total\ access-\min accessMax\ access-\min access$$

Where,
Acce.total: Raster of averaged times
Acce.min.: Minimum value of Acce.total
Acce.max.: Maximum value of Acce.total.

Whereupon we obtained the model in percentage values for each area of coverage.

5. RESULTS AND DISCUSSION

5.1 Evacuation coverage areas (ECA)

The evacuation coverage areas (ECA) represent the area of influence of buildings or security points, based on mobilization times expressed by a polygon on the ground. These coverage areas were obtained based on the times of each of the previously determined scenarios. The value of the existing population within each evacuation coverage area, has been obtained based on the index of population density through the last census in 2010 and the information given by the municipality of Salinas (INEC, 2010). During the vacation period the population increases by some 100%, which is also expressed and calculated in the second index of population density (Table 3).

Table 3: Population density of Salinas.

Public	Amount (Persons)	Urban area (Km^2)	Population density ($Persons/Km^2$)
Residents	29.294	27,07	1082,22
Tourists	58.588	27,07	2164,47

Based on the the two scenarios with the delimited times of 7 minutes and 20 seconds and 8 minutes an 22 segundos, respectively, we determined some seven evacuation coverage areas each, one for each safety point (Fig. 8). Based on the polygons obtained, which represent evacuation coverage areas and by the rate of population density, the number of existing population has been calculated within each of these areas, both at the time of low and high population density (high season, weekends and holidays; Table 3, 4).

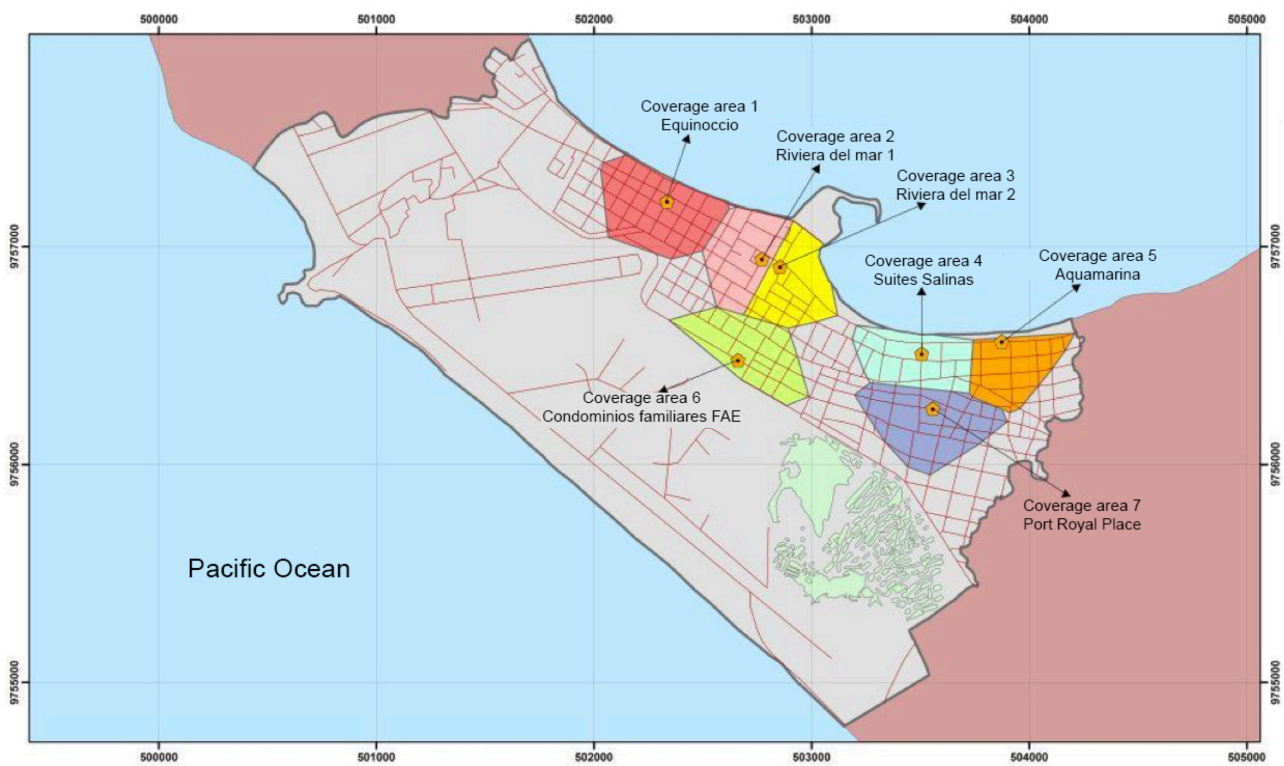

Fig. 8: The seven evacuation coverage areas (ECA), for the first scenario of Salinas.

Table 4 ECA attributes (first scenario) of Salinas.

Coverage area	Population (low season)	Population (high season)	Locations
ECA 1 - Equinoccio Building	196	392	Adapted
ECA 2 - Riviera del Mar 2	134	268	Adapted
ECA 3 - Riviera del Mar 1	132	264	Adapted
ECA 4 - Suites Salinas	141	281	Adapted
ACE 5 - Aquamarina Building	123	247	Adapted
ECA 6 - Condominios FAE	157	314	Adapted
ECA 7 - Port Royal Place	193	385	Insufficient (high season)

Table 5: ECA attributes obtained for the second scenario of Salinas.

As

Coverage area	Population (low season)	Population (high season)	Locations
ECA 1 - Equinoccio Building	237	474	Adapted
ECA 2 - Riviera del Mar 2	145	290	Adapted
ECA 3 - Riviera del Mar 1	147	294	Adapted
ECA 4 - Suites Salinas	179	359	Adapted
ACE 5 - Aquamarina Building	123	247	Adapted
ECA 6 - Condominios FAE	187	374	Adapted
ECA 7 - Port Royal Place	214	429	Insufficient (high season)

As the value of the population density has been calculated based on the urban area, a polygon within the study area defined as vertical evacuation area for the city of Salinas has been taken into account (Fig. 9).

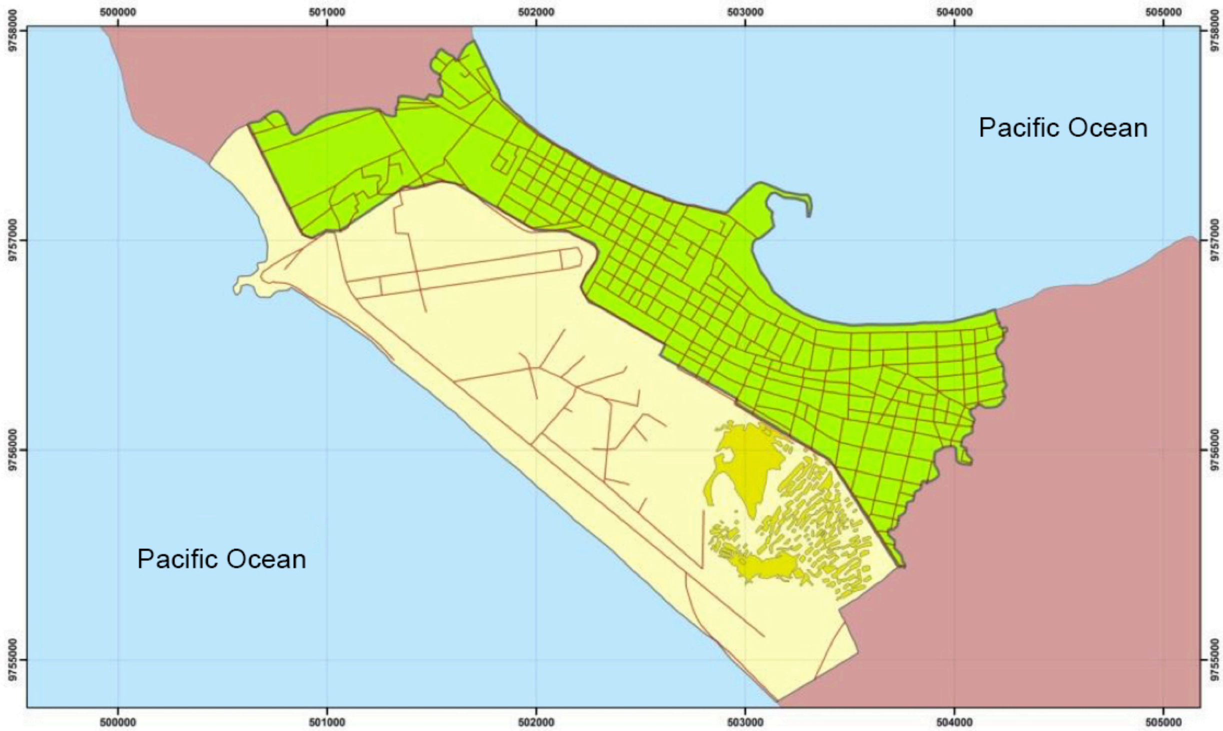

Fig. 9: Urban area (green) within the vertical evacuation zone of Salinas.

The urban area within the vertical evacuation zone covers a total of 2,241Km^2. The corresponding existing population value has been calculated within this zone and compared with the population which would be able to reach a safe area before it will affected by the first tsunami wave (Table 6).

Table 6: Calculated final amounts within the evacuation of Salinas.

Season	Indicadors	Scenario 7´20´´	Scenario 8´22´´
Low	Total population	2425	2425
	Evacuated persons	1076	1261
	Human loss	**1350**	**1164**
High	Total population	4851	4851
	Evacuated persons	2151	2522
	Human loss	**2699**	**2329**

Seven different models of accessibility for each specific scenario for the city of Salinas were obtained. To describe the results of accessibility three of the seven corresponding models are presented to each time scenario (Fig. 10; Table 7, 8).

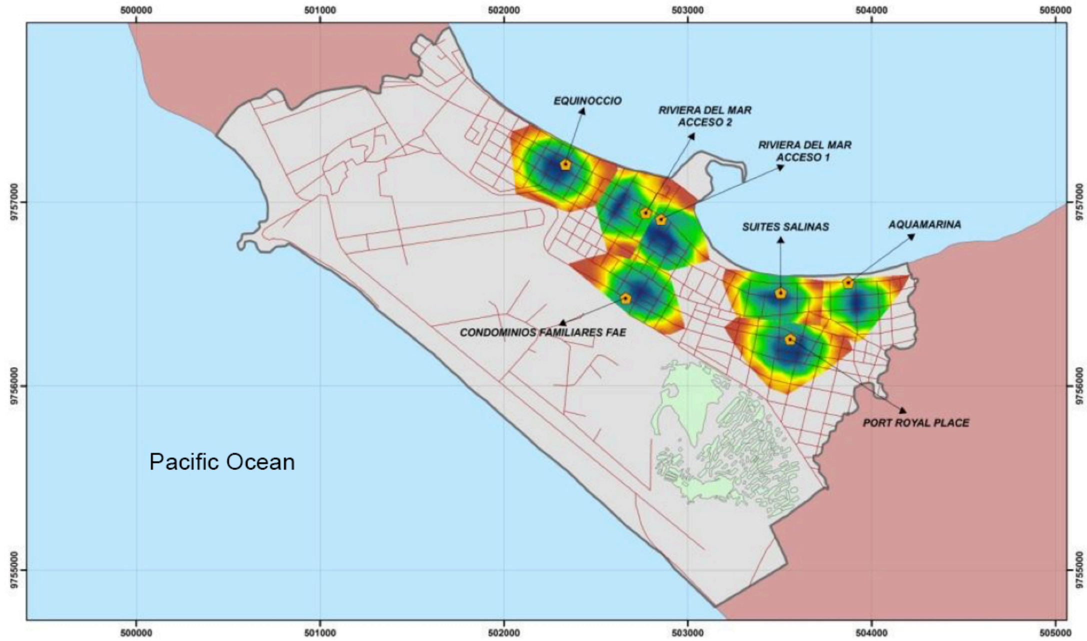

Fig. 10: Accessibility models for the first scenario of Salinas

Table 7: Description of the Accessibility Model for the first stage (scenario) of Salinas.

<table>
<tr>
<td>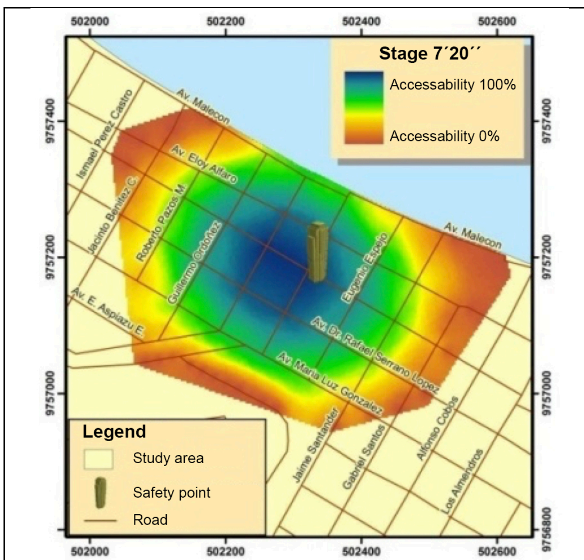
</td>
<td>EQUINOCCIO BUILDING

High values of accessibility reaching between 80% and 100% towards the center of the coverage area, specifically between the streets Guillermo Ordoñez and Eugenio Espejo. Low percentages between 0% and 20% were obtained in the extreme west, east and south of the coverage area.</td>
</tr>
</table>

<table>
<tr>
<td>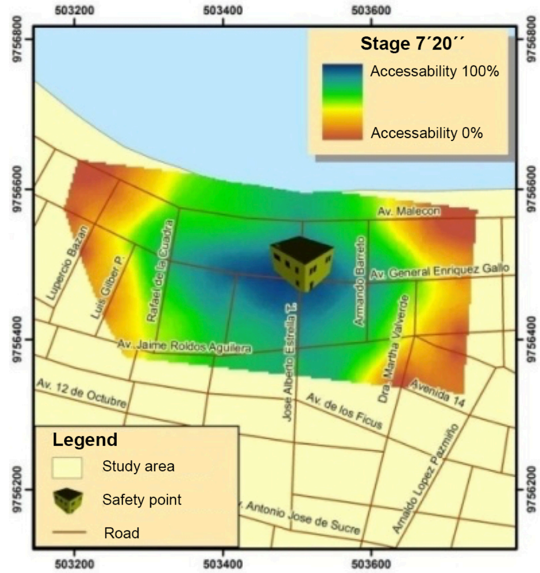
</td>
<td>

SUITES SALINAS

High values of accessibility were obtained being of up to 80% to 100% towards the center of the coverage area, specifically between te streets Rafael de la Cuadra and Armando Barreto. Low percentages between 0% and 20% were obtained in the extreme west and east of the coverage area.

</td>
</tr>
<tr>
<td>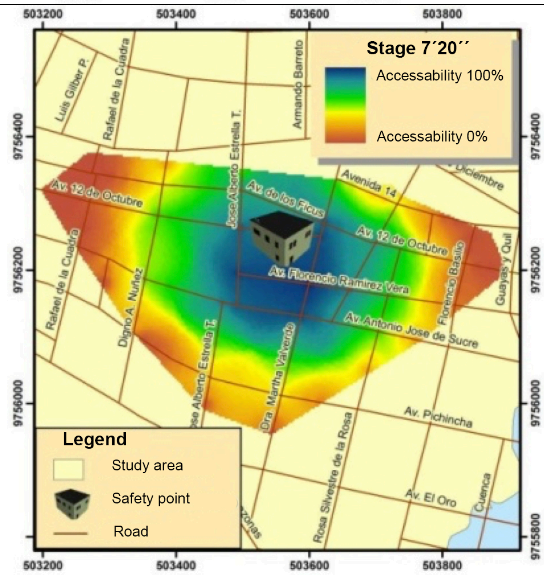
</td>
<td>

PORT ROYAL PLACE

High values of accessibility were obtained being of up to 80% to 100% towards the center of the coverage area, specifically between te streets José Alberto Estrella and Dra. Martha Valverde. Low percentages between 0% and 20% were obtained in the extreme west and east of the coverage area.

</td>
</tr>
</table>

The models obtained from the second scenario (stage) corresponding to 8 minutes 22 seconds has been very similar, with the difference that the coverage areas are extended ranging between 50 and 60 meters more, each.

5.2 Mobilization times

The mobilization is represented by the value of time it takes for a person to move from one initial point of evacuation to the nearest safety point, through the existing road network. Seven models of mobilization times for each of the two scenarios were determined for the City of Salinas, of which we have chosen to present three of them.

Table 8: Description of the mobilization model for the first stage (scenario) of Salinas.

<table>
<tr>
<td>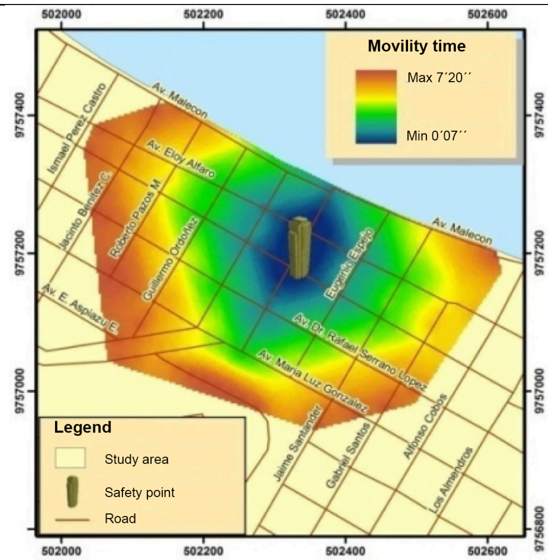
</td>
<td>EQUINOCCIO BUILDING

The lowest mobilization times were between 0'07" and 2'30" and are obviously within the area between the streets Pedro Jose Rodriguez and Eugenio Espejo. Consequently the highest times are in the remote areas related to the safety points.</td>
</tr>
<tr>
<td>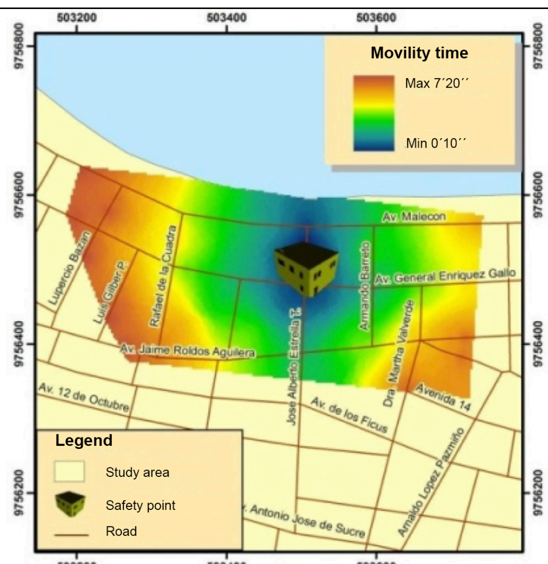
</td>
<td>SUITES SALINAS

The lowest mobilization times were between 0'07" and 2'30" and are obviously within the area between the avenues Malecón and General Enríquez Gallo. Therefore, the highest times are in the remote areas related to the safety points.</td>
</tr>
</table>

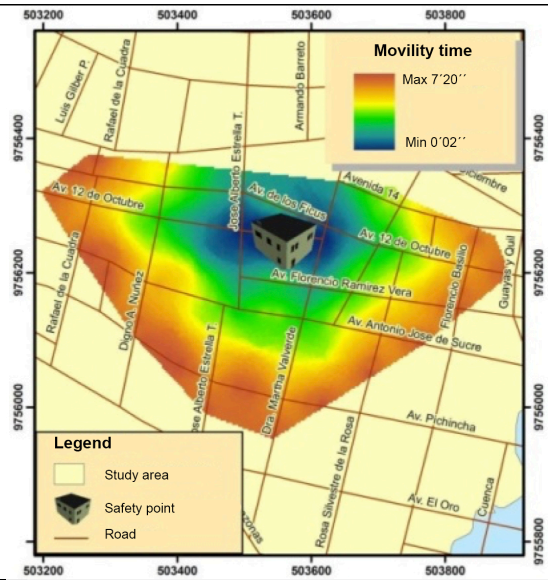

PORT ROYAL PLACE

The lowest mobilization times were between 0'07" and 2'30" and are obviously within the area between the streets de los Ficus and Florencio Ramírez. The highest times are in the remote areas related to the safety points.

According to the coverage areas of the second stage (scenario) corresponding to 8 minutes and 22 seconds, the obtained models are very similar, with the approximate addition of 1 further minute for every 60 meters on the road network.

5.3 Evacuation routes

The optimal evacuation routes are not necessarily the shortest, were obtained from the linear coverage mobilization times. With this coverage we determined the route with their respective mobilization time from any initial evacuation point to the safety point. We obtained seven models of evacuation routes for the most critical scenario (7'20") of the city of Salinas, of which we have chosen to present three representative examples.

Table 9: Description of the evacuation route model for the first stage (scenario) of Salinas.

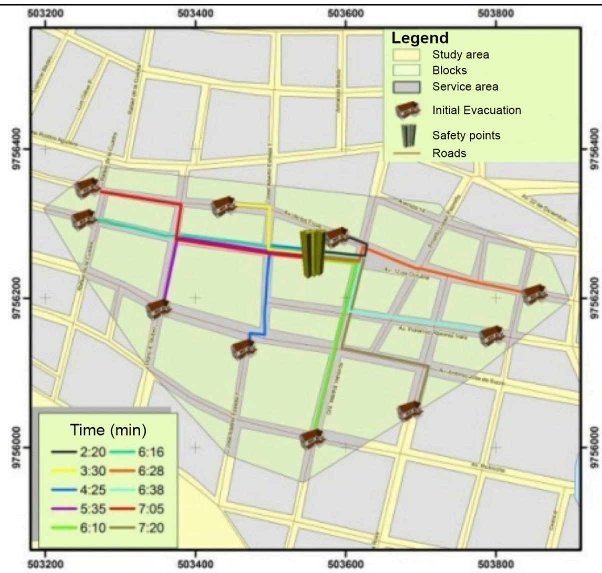	**EDIFICIO EQUINOCCIO** With a maximum time span for an evacuation of 7'20" the amount of evacuation points is considerable. However, road access and proper building entrances allow suitable conditions to facilitate the evacuation.
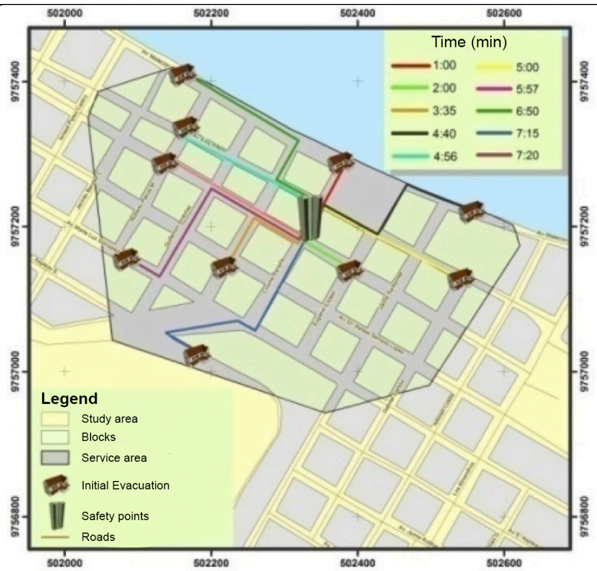	**SUITES SALINAS** With a maximum time span for an evacuation of 7'20" the amount of evacuation points is also in this example considerable. The road access and proper building entrances allow suitable conditions to facilitate the evacuation.

PORT ROYAL PLACE

Identical conditions like in the first two examples. Nonetheless, being an unfinished building, still in construction, its lower access and sites may be modified, so that evacuation allows to be optimal.

In the case of the second scenario (8'22") determined for the city of Salinas, in the same way we are able to determine the optimal route from any initial evacuation point to the safety point of each evacuation coverage area.

6. CONCLUSIONS

For the purposes of this research, the worst case scenario has been taken into consideration, in which we incorporated variables that include the most unfavorable conditions that may arise, in order to calculate and determine a greater safety margin that allows to save a high amount of human lives possible. To narrow vertical evacuation areas, the calculated tsunami arrival times for Salinas were used based on previous studies.

The potential areas of vertical evacuation of Salinas, have a high density of buildings with heights over four floors, but unfortunately a very low percentage of them are constructed under the existing norms and standards of earthquake resistance. In addition, due to the proximity of these buildings, in case of of an earthquake occurrence, these circumstances raise the degree of damage between them.
Las áreas de cobertura de evacuación (ECA), de cada punto de seguridad, conjuntamente con el índice de densidad poblacional, nos permiten conocer el número de personas que podrían ser evacuadas a cada edificio.

The ECA of each safety point, together with the population density index, allow us to know the amount of people who will be able to be evacuated to each building. However, in some cases, the buildings have unfortunately insufficient space to accommodate all evacuated persons.
According to the accessibility maps and mobilization times obtained, those living in the areas closest to elevated safe areas are more likely to reach them considering the factors of time, impedance and accessibility but being pendent on street network conditions.

With models and coverage areas obtained we were able to determine the paths and optimal times from anywhere within the ECA towards the safety points.

ACKNOWLEDGMENTS

We thank the Municipality of Salinas and the Universidad de las Fuerzas Armadas ESPE for logistic and financial support.

REFERENCES

Beck, S.L. and Ruff, L.J., 1984: The rupture process of the great 1979 Colombia earthquake: evidence for the asperity model. J.Geophys. Res.89: 9281–9291

Chunga, K. and Toulkeridis, T. (2014). First evidence of paleo-tsunami deposits of a major historic event in Ecuador. J. Tsunami Soc. Int, 33: 55-69.

Collot, J.Y., Marcaillou, B., Sage, F., Michaud, F., Agudelo, W., Charvis, P., Graindorge, D., Gutscher, M.A. and Spence, G., 2004. Are rupture zone limits of great subduction earthquakes controlled by upper plate structures? Evidence from multichannel seismic reflection data acquired across the northern Ecuador–southwest Colombia margin. Journal of Geophysical Research: Solid Earth, 109(B11).

Daniell, J.E., F. Wenzel, and B. Khazai. 2010. The Cost of Historical Earthquakes Today – Economic Analysis since 1900 through the use of CATDAT. Paper presented at the Australian Earthquake Engineering Society 2010 Conference, Perth, Western Australia: 15 pp.

Dengler, L., 2005. The role of education in the national tsunami hazard mitigation program. In Developing Tsunami-Resilient Communities (pp. 141-153). Springer Netherlands.

Dominey-Howes, D. and Papathoma, M., 2007. Validating a tsunami vulnerability assessment model (the PTVA Model) using field data from the 2004 Indian Ocean tsunami. Natural Hazards, 40(1): 113-136.

Egbue, O. and Kellogg, J., 2010: Pleistocene to Present North Andean “escape”. Tectonophysics 489: 248-257.

FEMA 2008. Guidelines for Design of Structures for Vertical Evacuation from Tsunamis. Washington, D.C., Federal Emergency Management Agency.

FEMA, 2012. Tsunami Vertical evacuation FEMA P646, Available at: https://www.youtube.com/watch?v=_h26_DUKMzA.

Fraser, S., Leonard, G.S., Murakami, H. and Matsuo, I., 2012. Tsunami Vertical Evacuation Buildings–Lessons for International Preparedness Following the 2011 Great East Japan Tsunami. Journal of Disaster Research, 7: 446-457.

Gusiakov, V.K., 2005: Tsunami generation potential of different tsunamigenic regions in the Pacific. Marine Geology, 215, 1-2: 3-9.

Gutscher, M.A., Malavieille, J.S.L. and Collot, J.-Y., 1999: Tectonic segmentation of the North Andean margin: impact of the Carnegie ridge collision. Earth Planet. Sci. Lett. 168: 255–270.

INEC, 2010: Censo Nacional de Población y Vivienda. Quito: Instituto Ecuatoriano de Estadística y Censos.

Ioualalen, M., Ratzov, G., Collot, J. Y. and Sanclemente, E. (2011). The tsunami signature on a submerged promontory: the case study of the Atacames Promontory, Ecuador. Geophysical Journal International, 184(2), 680-688.

Johnston, D., Paton, D., Crawford, G.L., Ronan, K., Houghton, B. and Bürgelt, P., 2005. Measuring tsunami preparedness in coastal Washington, United States. In Developing Tsunami-Resilient Communities (pp. 173-184). Springer Netherlands.

Jonientz-Trisler, C., Simmons, R.S., Yanagi, B.S., Crawford, G.L., Darienzo, M., Eisner, R.K., Petty, E. and Priest, G.R., 2005. Planning for tsunami-resilient communities. Natural Hazards, 35(1), pp.121-139.

Kanamori, H. and McNally, K.C., 1982: Variable rupture mode of the subduction zone along the Ecuador–Colombia coast. Bull. Seismol. Soc. Am.72 (4): 1241–1253.

Kelleher, J.A., 1972: Ruptures zones of large South American earthquakes and some predictions. Journal of Geophysical Research, 77, 11: 2087-2103.

Kellogg, J.N. and Vega, V., 1995: Tectonic development of Panama, Costa Rica and the Colombian Andes: Constraints from Global Positioning System geodetic studies and gravity. Geol. Soc. Am. Special Paper 295, 75–90.

Mas, E., Adriano, B. and Koshimura, S., 2013. An integrated simulation of tsunami hazard and human evacuation in La Punta, Peru. Journal of Disaster Research, 8(2), pp.285-295.

Matheus, A., 2012. Modelo de evacuación vertical y horizontal en caso de ocurrencia de tsunami para las ciudades de Salinas y Bahía de Caráquez. Universidad de las Fuerzas Armadas ESPE. Unpublished Thesis, 195pp

Muhari, A., Koshimura, S. and Imamura, F., 2012. Performance evaluation of pedestrian bridge as vertical evacuation site during the 2011 tsunami in Japan. Journal of Natural Disaster Science, 34(1): 79-90.

NEC-15, 2015: Norma Ecuatoriana de la Construcción, SE-DS, Cargas Sísmicas. Diseño Sismo Resistente. Quito, Ecuador: 138pp.

Olsson, A.A., 1931. Contributions to the Tertiary paleontology of northern Peru: Part 4. The Peruvian Oligocene. Bull. Am. Pal., 17 (63): 100-264.

Padilla, O., Cruz D'Howitt, M. and Alvear Brito, J., 2009. Elaboración De Un Mapa De Accesibilidad Y Modelo De Evacuación Ante Una Eventual Ocurrencia De Tsunami En Las Ciudades De Salinas Y Bahía De Caráquez , Mediante Herramientas Geoinformáticas. Revista Geoespacial, 5: 1–15.

Pararas-Carayannis, G. 1980: The Earthquake and Tsunami of December 12, 1979, in Colombia. Intern. Tsunami Information Center Report, Abstracted article in Tsunami Newsletter, Vol. XIII, No. 1.

Pararas-Carayannis, G., 2012: Potential of tsunami generation along the Colombia/Ecuador subduction margin and the Dolores-Guayaquil Mega-Thrust. Science of Tsunami Hazards, 31, 3: 209-230.

Park, S., Van de Lindt, J.W., Gupta, R. and Cox, D., 2012. Method to determine the locations of tsunami vertical evacuation shelters. Natural hazards, 63(2), pp.891-908.

Pontoise, B. and Monfret, T. (2004). Shallow seismogenic zone detected from an offshore‐onshore temporary seismic network in the Esmeraldas area (northern Ecuador). Geochemistry, Geophysics, Geosystems, 5(2).

Raschky, P.A. 2008. Institutions and the losses from natural disasters. Natural Hazards and Earth System Science 8: 627-634.

Ratzov, G., Collot, J. Y., Sosson, M. and Migeon, S. (2010). Mass-transport deposits in the northern Ecuador subduction trench: Result of frontal erosion over multiple seismic cycles. Earth and Planetary Science Letters, 296(1), 89-102.

Ratzov, G., Sosson, M., Collot, J. Y., Migeon, S., Michaud, F., Lopez, E. and Le Gonidec, Y. (2007). Submarine landslides along the North Ecuador–South Colombia convergent margin: possible tectonic control. In Submarine Mass Movements and Their Consequences. Springer Netherlands: 47-55

Reese, S., Cousins, W. J., Power,W. L., Palmer, N. G., Tejakusuma, I. G., and Nugrahadi, S., 2007: Tsunami vulnerability of buildings and people in South Java field observations after the July 2006 Java tsunami, Nat. Hazards Earth Syst. Sci., 7, 573–589.

Rodriguez, F., DHowitt, M.C., Toulkeridis, T., Salazar, R., Romero, G.E.R., Moya, V.A.R. and Padilla, O., 2016. Journal of Tsunami Society International. Journal of Tsunami Society International, 35(1).

Rudolph E. and Szirtes S., 1911: Das kolumbianische Erdbeben am 31 Januar 1906, Gerlands Beitr. z. Geophysik , 2: 132- 275.

Senn, A., 1940. Paleogene of Barbados and its bearing on history and structure of Antillean-Caribbean region. AAPG bulletin, 24(9), pp.1548-1610.

Shepperd, G.L. and Moberly, R., 1981: Coastal structure of the continental margin, northwest Peru and southwest Ecuador. Geological Society of America Memoirs, 154: 351-392,

Steinmetz, T., Raape, U., Teßmann, S., Strobl, C., Friedemann, M., Kukofka, T., Riedlinger, T., Mikusch, E. and Dech, S., 2010. Tsunami early warning and decision support. Natural Hazards and Earth System Sciences, 10(9), pp.1839-1850.

Swenson, J.L. and Beck, S.L., 1996: Historical 1942 Ecuador and 1942 Peru subduction earthquakes, and earthquake cycles along Colombia–Ecuador and Peru subduc-tion segments. Pure Appl. Geophys.146 (1): 67–101.

Taubenböck, H., Goseberg, N., Setiadi, N., Lämmel, G., Moder, F., Oczipka, M., Klüpfel, H., Wahl, R., Schlurmann, T., Strunz, G. and Birkmann, J., 2009. " Last-Mile" preparation for a potential disaster–Interdisciplinary approach towards tsunami early warning and an evacuation information system for the coastal city of Padang, Indonesia. Natural hazards and earth system sciences, 9(4), pp.1509-1528.

Toulkeridis et al., 2016a: Real-Time Radioactive Precursor of the April 16, 2016 Mw 7.8 Earthquake in Ecuador. Submitted

Toulkeridis et al., 2016b: The 7.8 Mw Earthquake and Tsunami of the 16th April 2016 in Ecuador - A seismic evaluation and geological field survey. Submitted

Toulkeridis, 2011: Volcanic Galápagos Volcánico. Ediecuatorial, Quito, Ecuador: 364 pp

Velotti, L., Trainor, J.E., Engel, K., Torres, M. and Myamoto, T., 2013. Beyond vertical evacuation—research considerations for a comprehensive vertical protection strategy. International Journal of Mass Emergencies and Disasters, 31(1), pp.60-77.

Walters, R.A. and Goff, J., 2003. Assessing tsunami hazard along the New Zealand coast. Science of Tsunami Hazards, 21(3), pp.137-153.

Wood, N., Jones, J., Schelling, J. and Schmidtlein, M., 2014. Tsunami vertical-evacuation planning in the US Pacific Northwest as a geospatial, multi-criteria decision problem. International journal of disaster risk reduction, 9, pp.68-83.

Xie, J., Nistor, I. and Murty, T., 2012. Tsunami risk for Western Canada and numerical modelling of the Cascadia fault tsunami. Natural hazards, 60(1), pp.149-159.

Yeh, H.H.J., Robertson, I. and Preuss, J., 2005. Development of design guidelines for structures that serve as tsunami vertical evacuation sites (Vol. 4). Washington State Department of Natural Resources, Division of Geology and Earth Resources.